Vol. 12 No. 3, 2026
Baltic Journal of Economic Studies
DOI: https://doi.org/10.30525/2256-0742/2026-12-3-1-17

COORDINATING HOUSEHOLD DEMAND AND VEHICLE-USE ARCHETYPES TO ENABLE URBAN ON-STREET EV CHARGING WITHOUT DISTRIBUTION UPGRADES

Aivars Rubenis[1], Aigars Laizans[2], Girts Aleksans[3]

Abstract. Urban electrification strategies are increasingly relying on on-street charging to support residents without private driveways. However, distribution networks in dense neighbourhoods often operate near the limits established during their initial planning. This paper uses Kensington, London, as an example to focus on on-street charging in medium-density urban areas with terraced housing, and to investigate whether coordinated, phase-aware charging can increase EV uptake in multi-occupancy residential settings without triggering costly network reinforcement. Specifically, the study quantifies the impact of household demand stochasticity and vehicle-use heterogeneity on available thermal headroom and charging adequacy, as defined by standard After Diversity Maximum Demand (ADMD) planning levels. The analysis integrates a high-resolution residential demand model with behavioural EV driving archetypes to simulate overnight charging over a 365-day period, utilising the existing grid connection of six flat terraced houses without grid updates. The model employs ADMD to define aggregate feeder capacity and to simulate scenarios in which total load is managed to prevent exceeding the per-household diversified rating. The framework evaluates the sufficiency of the morning state of charge (SoC) for one, two or three vehicles by comparing an optimised phase-balancing strategy with a worst-case uncoordinated allocation. The results demonstrate that, for a six-flat terraced house, the available "soft" ADMD headroom, which is dictated by the coincidence of household base load, is the primary binding constraint rather than charger nameplate power. For initial uptake of one EV per six flats, the mean morning battery SoC remains high (70–73%). However, as the number of vehicles increases to three per shared constraint, the system reaches a capacity-saturated regime. In this state, optimisation improves grid quality and prevents localised phase overloads, but cannot offset the overall energy deficit. These findings suggest that, although phase-aware coordination can facilitate early-stage on-street electrification, saturation levels will require either physical reinforcement or advanced demand flexibility.

Keywords: smart EV charging, on-street charging access inequality, after-diversity maximum demand (ADMD), three-phase phase balancing, EV charging control.

JEL Classification: C61, Q41, Q48, R41, R48

1. Introduction

The European Union (EU) is working to build an energy system that produces far less carbon and is more resilient to disruption. Key policies, including the European Green Deal and related strategies, aim to achieve climate neutrality by 2050. One of the primary conditions for meeting this target is reducing greenhouse gas emissions from passenger cars (European Climate Law, 2021). A resilient energy infrastructure that can withstand external shocks while remaining affordable is essential for achieving this goal (European Commission, 2025).

While research and the charging industry have focused primarily on fast charging until recently, interest is increasingly shifting towards on-street charging. This reflects the practical needs of urban residents who lack private driveways, particularly in countries where a large proportion of the population lives in cities and various solutions to this problem are being sought (Office for Zero Emission Vehicles, 2025). It also highlights the need for more research into the potential impact on the electricity grid and the practical implementation of large-scale infrastructure rollout in urban areas.

[1] Latvia University of Life Sciences and Technologies, Latvia *(corresponding author)*
E-mail: aivars.rubenis@ivorygroup.eu
ORCID: https://orcid.org/0000-0001-8765-7790
[2] Latvia University of Life Sciences and Technologies, Latvia
ORCID: https://orcid.org/0000-0002-2352-5921
[3] PC Consulting, SIA, Latvia

Existing literature on electric vehicle (EV) charging using residential electricity connections shows that smart, coordinated charging is feasible and can mitigate grid constraints, particularly in low-voltage networks. Optimisation techniques, including two-stage algorithms and real-time water-filling, have the potential to reduce peak demand and costs without compromising user needs (Sastry et al., 2023). Economic analyses reveal that such strategies could lower demand charges by 20–35% at moderate EV penetration levels and increase self-consumption in PV-integrated residential setups (Zhang et al., 2017; Tveit et al., 2022). However, studies tend to focus on either single-family homes or neighbourhood-level systems. There is limited direct evidence on urban on-street charging for households without private driveways. Furthermore, stochastic modelling of parking and charging windows is under-explored. This suggests a need for further research in dense urban contexts (Anadón Martínez & Sumper, 2023; Doda et al., 2024).

Although these studies prioritise optimisation and demand response, applications are often generalised to residential or LVDS settings rather than to specific urban, on-street scenarios where shared connections could exacerbate constraints (Sastry et al., 2023; Tveit et al., 2022; Teawnarong et al., 2024).

Coordinated charging strategies are essential for managing EV loads on existing residential electricity connections, particularly in areas where there are limits on low-voltage network capacity. A two-stage smart charging algorithm optimises EV charging for single-family residences first from the owner's perspective, minimising costs via price signals, and then adjusting among multiple optimal solutions to reduce grid impacts such as voltage violations and equipment stress (Sastry et al., 2023). Evaluated through Monte-Carlo simulations on a physics-based distribution feeder model, this decentralised approach shows that, without coordination, smart charging based solely on price minimisation can mimic the adverse effects of rapid, unrestricted charging, such as peak overloads.

In low-voltage distribution systems (LVDS), a local energy market (LEM) framework coordinates electric vehicle (EV) charging among prosumers and owners. It uses optimisation to select transaction partners and negotiate prices, while also enforcing distribution network constraints (DNCs) (Teawnarong et al., 2024).

Although stochastic modelling is employed to capture uncertainties in EV use and infrastructure availability, direct focus on parking or on-street charging windows remains sparse. In smart charging assessments for residential areas, Monte-Carlo simulations are used to model EV adoption scenarios, incorporating stochastic elements such as charging start times and durations derived from real-world patterns (Sastry et al., 2023). A survey of Danish electric vehicle (EV) owners identified three archetypal charging patterns (e.g., frequent short sessions vs. overnight), which were integrated into optimisation models to simulate flexibility (Tveit et al., 2022). This empirical load-shape analysis takes into account stochastic connection times and availability, demonstrating that strategies that respond to price or PV output are most effective when EVs connect during periods of high opportunity, such as evenings or sunny periods. However, the models are based on private connections, which limits the insight they provide into variability in on-street parking in urban areas without driveways.

While broader reviews acknowledge the necessity of stochastic programming for public charging planning, including archetype models for vehicle usage and parking availability to predict potential timeframes (Anadón Martínez & Sumper, 2023), there is a lack of empirical studies on the feasibility of urban on-street charging (Anadón Martínez & Sumper, 2023; Doda et al., 2024). Further research is required to develop these into archetype-based simulations of street parking turnover and shared connection access.

Techno-economic optimisation at the level of individual households or neighbourhoods evaluates the viability of EV charging on existing connections by minimising costs and emissions. For residential PV-EV systems, optimisation involves comparing the costs and self-consumption of different charging strategies. The results show that price- and emission-based signals reduce expenses, whereas PV-focused strategies increase the use of renewable energy (Tveit et al., 2022). Net present cost (NPC) analyses in microgrid contexts, such as PV-retrofitted car parks (which can be adapted for neighbourhood lots), confirm the economic feasibility of high-irradiation areas, with NPC savings of 8-16% via coordinated scheduling (Ivanova et al., 2020). Economic analyses indicate that smart charging on existing residential connections is feasible and cost-effective, particularly with optimisation. Demand charge reductions and welfare maximisation offset the need for grid upgrades, with EVs enabling revenue through flexibility services (Zhang et al., 2017; Teawnarong et al., 2024). In homes with PV integration, strategies that align charging with low-cost periods yield positive financial impacts, though achieving full self-sufficiency depends on connection frequency (Tveit et al., 2022).

For urban on-street charging, which is critical for households without driveways, the feasibility of coordinated access to shared connections is key. However, the available literature only provides indirect insights. Planning reviews emphasise the importance of collaboration between public infrastructure operators and grids, with economic models favouring decentralised optimisation to prevent overloading (Anadón Martínez & Sumper, 2023). Smart city integrations highlight cost savings through ML-driven demand response. However, economic implications, such as equitable tariffs for on-street users, remain

under-explored (Doda et al., 2024). Challenges include higher initial coordination costs and variable parking. This suggests that stochastic models could quantify the benefits, such as operational savings of 11–16% in retrofit scenarios (Ivanova et al., 2020).

It is evident that, while optimisation and empirical analyses affirm feasibility in residential contexts, further empirical studies are required on shared low-voltage economics and stochastic parking archetypes in urban on-street contexts, in order to address adoption barriers.

2. Methods

2.1. Conceptual Structure of the Modelling Framework

This study has developed an analytical framework designed to assess the feasibility of large-scale on-street electric vehicle (EV) electrification in dense urban residential environments, eliminating the need for local distribution grid reinforcements. The model is structured as a multi-layer, bottom-up system in which behavioural demand, mobility needs, charging activity and electrical constraints are explicitly represented and integrated through consistent temporal resolution.

At its core, the framework is not one optimisation problem, but rather a hierarchically coupled set of sub-models, each of which addresses a distinct physical or behavioural dimension of the system. This modular design means that individual components can be empirically validated, replaced, or extended without altering the overall structure. This separation is particularly important in the context of urban electrification, where uncertainties in user behaviour, vehicle availability and policy constraints interact non-linearly.

The modelling framework consists of four interconnected layers: residential electricity demand, vehicle usage and charging demand, on-street charging infrastructure allocation, and local electricity system interaction. Each layer functions at an hourly temporal resolution and is defined consistently over a shared annual simulation horizon.

2.2. Mathematical Formalisation and Time Indexing

Time discretisation and horizon

The integrated model is defined over a discrete-time annual horizon with a uniform time step. Let the set of time intervals be $t \in \mathcal{T} = \{1, 2, \ldots, T\}$, where each interval corresponds to one hour and $T = 8,760$ for a non-leap year. This hourly index consistently represents all electricity quantities to preserve the diurnal residential demand structure and capture the coincidence between residential peaks and feasible overnight charging windows.

Building, dwelling, and phase indices

The analysis is conducted for a representative multi-occupancy converted terraced house in London, the Kensington and Chelsea area, which is treated as a single building entity indexed by b. The building contains a set of dwellings (flats) indexed by $f \in \mathcal{F}$. Each dwelling is assumed to be supplied as a single-phase customer, while the building intake is represented as a three-phase low-voltage connection. The set of phases is therefore indexed by $\phi \in \Phi = \{A, B, C\}$.

A fixed phase-assignment mapping $a : \mathcal{F} \to \Phi$ is used to represent which intake phase supplies each dwelling. This mapping is purely electrical in nature and is treated as exogenous within the accounting framework.

Baseline residential demand and phase aggregation

Let $D_{f,t}$ denote the baseline residential electricity demand of a dwelling f at time t, excluding any EV charging demand. By construction, $f \in \mathcal{F}$ for all $f \in \mathcal{F}$ and $t \in \mathcal{T}$. The phase-level baseline demand is obtained by summing the demands of dwellings allocated to the respective phase:

$$D_{\phi,t} = \sum_{f \in \mathcal{F}: a(f) = \phi} D_{f,t}, \text{ for all } \phi \in \Phi \text{ and } t \in \mathcal{T}. \quad (1)$$

The building-level baseline demand is then defined as the sum across phases:

$$D_{b,t} = \sum_{\phi \in \Phi} D_{\phi,t}, \text{ for all } t \in \mathcal{T}. \quad (2)$$

At this stage, $D_{f,t}$ is treated as an exogenous time series. The empirical construction of representative demand shapes and the justification for scaling magnitudes without altering the diurnal structure will be introduced later. This draws on the well-established finding that normalised residential load shapes remain stable across consumption levels in multi-apartment contexts.

Intake capacity parameters

Let V^{nom} denote the nominal phase-to-neutral voltage at the building intake. Define $I_{\phi}^{\max}$ as the current limit on the phase ϕ at the intake, reflecting the service-fuse rating or an equivalent maximum import threshold. The corresponding maximum import power per phase is defined as:

$$P_{\phi}^{\max} = V^{\text{nom}} \cdot I_{\phi}^{\max}, \text{ for all } \phi \in \Phi. \quad (3)$$

The building's total maximum import capacity is defined as the sum of per-phase limits:

$$P_{b}^{\max} = \sum_{\phi \in \Phi} P_{\phi}^{\max}. \quad (4)$$

Such limits, including supplies up to 100 A per phase, are characterised in UK DNO engineering guidance for LV customer supplies (UK Power Networks, 2025b).

EV charging load representation

Let $P_{\phi,t}^{\mathrm{EV}}$ denote the EV charging power drawn on phase ϕ at time t. This quantity aggregates all EV charging processes that are electrically connected to phase ϕ during interval t. Phase-wise total electrical load is therefore defined as:

$$L_{\phi,t} = D_{\phi,t} + P_{\phi,t}^{\mathrm{EV}}, \text{ for all } \phi \in \Phi \text{ and } t \in \mathcal{T}. \quad (5)$$

The corresponding building total load is:

$$L_{b,t} = \sum_{\phi \in \Phi} L_{\phi,t}, \text{ for all } t \in \mathcal{T}. \quad (6)$$

This representation distinguishes between EV charging demand and the mechanism that schedules it. Consequently, no assumptions have yet been made regarding plug-in times, charging rates, phase-switching logic or smart-charging behaviour.

Per-phase headroom as the core feasibility identity

A central object for subsequent feasibility assessment is the residual capacity (headroom) between the per-phase import limit and the realised phase load. This is an accounting identity, as defined by the relevant authorities:

$$R_{\phi,t} = P_{\phi}^{\max} - L_{\phi,t}, \text{ for all } \phi \in \Phi \text{ and } t \in \mathcal{T}. \quad (7)$$

Positive values of $R_{\phi,t}$ indicate unused phase capacity at time t. Negative values indicate that the combined baseline and EV charging load exceeds the phase import limit and would be infeasible unless EV charging were rescheduled, curtailed, or otherwise reallocated. In this section, $R_{\phi,t}$ is defined only as a descriptive measure; it becomes a binding constraint only once charging-allocation rules are introduced.

2.3. Electricity Demand Submodule

The electricity demand submodule provides the baseline residential load process $D_{f,t}$ for each dwelling f in the representative Cornwall Gardens, Kensington building and, by aggregation, the phase-resolved baseline loads $D_{\phi,t}$ required by the accounting identities introduced in Section 3.2. The submodel is designed to preserve the intra-day and seasonal structure of household electricity use that has been empirically observed, while scaling consumption magnitudes to levels appropriate for the dwellings in the case study. This approach is based on the recent findings that, once normalised, diurnal load shapes in multi-apartment contexts exhibit limited systematic variation across consumption levels (Rubenis & Laizans, 2026). This implies that differences in annual demand are primarily due to scale rather than to fundamentally different daily routines.

Data source and harmonisation to the model time index

The baseline household electricity consumption data was derived from the smart meter dataset released by the Low Carbon London programme, led by UK Power Networks and made available via the London Datastore (UK Power Networks, 2014). The dataset contains half-hourly electricity consumption readings (kWh per half-hour), an anonymised household identifier, and timestamps, covering a sample of 5,567 households observed between November 2011 and February 2014, which is documented in detail by (Schofield et al., 2015). These households are subject to standard fixed-rate tariffs, which apply a uniform unit price alongside a daily standing charge. They receive no monetary incentives to modify their energy consumption.

Because the integrated framework in Section 2.2 is defined on an hourly time index $t \in \mathcal{T}$, the half-hourly observations are harmonised to hourly resolution by aggregation. Let $E_{h,\tau}^{(30)}$ denote the recorded consumption (kWh) for a household h in a half-hour interval τ. Hourly consumption $D_{h,t}^{\mathrm{raw}}$ is constructed as

$$D_{h,t}^{\mathrm{raw}} \Big| = \Big| E_{h,2t-1}^{(30)} + E_{h,2t}^{(30)}, \quad (8)$$

ensuring that the resulting series is energy-consistent and directly comparable to the hourly quantities used elsewhere in the model.

Any missing or anomalous readings are dealt with in a conservative manner to prevent peaks that are relevant to capacity assessment from being smoothed out artificially. Periods with insufficient data coverage are excluded from the construction of profiles.

Construction of representative demand shapes

The purpose of the demand submodule is to generate a set of empirically grounded baseline load profiles that can be scaled and combined to represent multiple flats within a modelled building. The central modelling step is therefore the separation of each household's demand into two components: (i) a normalised shape component that captures timing and relative variation, and (ii) a scale component that determines annual magnitude.

For each household h., define annual consumption over the available observation window as

$$A_h \Big| = \Big| \sum_{t \in \mathcal{T}_h} D_{h,t}^{\mathrm{raw}}, \quad (9)$$

where $\mathcal{T}_h$ is the set of valid hourly intervals retained after data-quality filtering. The corresponding normalised load shape is defined as

$$s_{h,t} \Big| = \Big| \frac{D_{h,t}^{\mathrm{raw}}}{A_h}, t \in \mathcal{T}_h, \quad (10)$$

so that $\sum_{t \in \mathcal{T}_h} s_{h,t} = 1$. This normalisation puts all households on an equal footing and removes the effects of time of day and seasonality from differences in overall consumption levels.

In the context of the recent study (Rubenis & Laizans, 2026), which established that normalised diurl

profiles remain largely consistent across consumption bands in multi-apartment settings, the present paper hypothesises that the normalised shape can be transferred across households. The paper proposes that dwelling-level heterogeneity is primarily represented through scaling and stochastic sampling of shapes, rather than through separate behavioural regimes.

Specifically, the set of candidate household shapes $\{s_{h,t}\}$ is restricted to those whose annual consumption falls within a range consistent with the target dwelling characteristics of the Kensington case, and a sample of these shapes is then used to represent the flats within the building.

2.4. Vehicle Usage and Charging-Demand Submodule

Vehicle usage archetypes

This submodule translates heterogeneous vehicle-use behaviour into an exogenous charging-energy requirement and a set of admissible charging opportunity windows. Collectively, these form the behavioural input to the feasibility assessment. The modelling unit is an archetype $\mathrm{n} \in \mathcal{K}$, interpreted as a behavioural primitive that summarises statistically distinct mobility patterns. In line with the archetype methodology developed by Rubenis, Tonova et al. (2025), the archetype profiles are considered to be empirical representations of driving intensity and temporal availability in reduced form.

For each archetype *k*, an activity schedule is defined, distinguishing between driving intervals and parked intervals. This schedule is utilised to construct two objects that are imperative for conducting a charging feasibility analysis. Firstly, an energy-withdrawal process associated with driving activity is required. Secondly, an availability process that specifies when charging could occur because the vehicle is stationary.

Energy-demand construction

The energy demand model has been formulated in (Rubenis, Laizans, et al., 2025). For each day d and archetype k, the model uses daily aggregate mobility descriptors as inputs: total driving distance $D_{d,k}$ (km) and total driving time $T_{d,k}$ (h). Daily average speed is defined as $v_{d,k} = D_{d,k} / T_{d,k}$ for $T_{d,k} > 0$; for non-driving days, daily traction energy is zero by definition.

The specific traction energy consumption is constructed as an interpolation between an urban benchmark s_{city} and a combined (higher-speed) benchmark s_{comb}. The interpolation weight is defined by a logistic function $w(v_{d,k})$ that decreases smoothly from near one at low speeds to near zero at higher speeds, with parameters selected such that the midpoint occurs at approximately 55 km/h.

Daily driving energy demand (kWh) is then computed as the sum of traction energy and auxiliary energy:

$$E_{d,k} = s_{eff}\left(v_{d,k}\right) D_{d,k} + \gamma_{aux}\left(\theta_d\right) T_{d,k} \quad (11)$$

The first term represents traction energy proportional to distance, while the second term represents auxiliary consumption associated with heating, ventilation, and air conditioning, expressed as a temperature-dependent power requirement $\gamma_{\text{aux}}(\theta_d)$ applied over driving time.

For later integration into the hourly accounting framework, daily energy demand $E_{d,k}$ is interpreted as the energy that must be replenished through charging over feasible parked intervals associated with the same day (or, when required, across adjacent days), subject to the charging allocation mechanism introduced in subsequent submodels.

Vehicle availability and charging opportunity windows

Charging feasibility depends not only on the magnitude of $E_{d,k}$, but also on whether sufficient parked time exists to deliver this energy given infrastructure power limits and local electrical headroom. Let $A_{k,t}$ denote an availability indicator, where $A_{k,t} = 1$ implies that the archetype vehicle is parked and could, in principle, be connected to on-street residential charging infrastructure at time t, and $A_{k,t} = 0$ implies that the vehicle is driving and cannot charge.

In this paper, $A_{k,t}$ is treated as exogenous and archetype determined. The model therefore constructs, for each day, a feasible set of possible charging hours:

$$\mathcal{T}_{d,k}^{chg} \subseteq \mathcal{T} \text{ such that } t \in \mathcal{T}_{d,k}^{chg} \text{ only if } A_{k,t} = 1. \quad (12)$$

This object can be regarded as the behavioural interface between mobility and charging; it identifies when charging could occur, without yet specifying how charging is scheduled within that set.

Outputs passed to the feasibility assessment

The submodule yields two outputs that are required by subsequent layers of the integrated framework. First, it produces archetype-indexed daily energy requirements $E_{d,k}$, derived from observed mobility quantities using the WLTP-calibrated mapping above. Second, it produces archetype availability indicators $A_{k,t}$ (and equivalently, possible charging hour sets $\mathcal{T}_{d,k}^{\text{chg}}$), which define the admissible temporal domain over which the required energy can be delivered.

2.5. On-Street Residential Charging Infrastructure Submodule

This subsection defines the representation of on-street charging infrastructure that mediates between vehicle availability and the electricity system interaction layer. It does not yet impose network headroom constraints or any optimisation logic. It specifies the charging assets and their electrical

interface characteristics, as well as the admissible operating states, which are subsequently evaluated against the phase-resolved import limits.

Charger set and operating variables

Let $c \in \mathcal{C}$ index on-street charging points that serve the representative building's residents. Each charger is characterised by a rated maximum active power $P_c^{\max}$ (kW), the charging efficiency β and an availability state that reflects whether it is occupied by a vehicle. Charging is represented by an hourly power draw variable $P_{c,t}^{\text{chg}}$ (kW), defined for all $t \in \mathcal{T}$ and bounded by the physical rating:

$$0 \le P_{c,t}^{chg} \le P_c^{max}. \quad (13)$$

The model treats $P_{c,t}^{\text{chg}}$ as the electrical power drawn at the charger terminals. Energy delivered in hour t is therefore $E_{c,t}^{\text{chg}} = P_{c,t}^{\text{chg}} \cdot \beta \cdot \Delta t$, with $\Delta t = 1$ hour under the discretisation introduced previously.

Electrical interface and representative power levels

The infrastructure is modelled on AC conductive charging equipment, which is consistent with the international EV supply equipment standard. In this system, the charging point provides controlled AC power and communicates with the vehicle to enforce safe current limits. The IEC defines the general requirements for EV supply equipment in IEC 61851-1, which applies to AC and DC EV charging equipment up to specified voltage limits (International Electrotechnical Commission, 2017).

In the context of London's kerbside infrastructure, slow AC charging power is typical. As an empirical reference point for representative infrastructure capability, Ubitricity's on-street lamp-post and bollard equipment, which has been deployed on a large scale, reports a standard maximum charging capacity of approximately 3.6–5 kW (single-phase, 16–25 A at nominal 230 V) for its lamppost-based solution (Ubitricity, 2025). The submodel therefore allows $P_c^{\max}$ to be set to technology-representative values, while keeping the formal structure general so that alternative equipment ratings can be tested later through parameterisation rather than by altering model logic.

Connection state, session feasibility, and deliverable energy

Charging can occur only when a vehicle is both available to charge (as defined by the archetype availability indicator $A_{k,t}$ in Section 2.4) and physically connected to a charger. Let $x_{c,k,t}$ be an indicator that equals 1 if a vehicle of archetype k occupies charger c during hour t, and 0 otherwise. The infrastructure feasibility conditions are then expressed as:

– As each charger can serve only one vehicle at a time, the total occupancy over all archetypes for each charger and hour is bounded by one.

– charging power is permitted only when a charger is occupied, so $P_{c,t}^{\text{chg}}$ is constrained to be zero whenever the charger is not occupied.

For each archetype k, the total energy delivered through all chargers during a day must be sufficient to satisfy the archetype's replenishment requirement $E_{d,k}$ derived in Section 2.4, subject to the availability windows and infrastructure capacity. At the accounting level, this is represented by aggregating the delivered energy at charger level over the relevant hours and equating it to the required daily replenishment.

Phase attachment and phase-switching capability

As the upstream intake is three-phase and charging points are usually single-phase, each charger must be connected to one phase only at any given time. Let $\phi(c,t) \in \{A,B,C\}$ denote the phase to which charger c is connected in hour t. Two modelling regimes are distinguished.

In the fixed-phase regime, $\phi(c,t)$ is time-invariant and reflects a static wiring choice. In the dynamic-phase regime, $\phi(c,t)$ may vary over time, representing a phase-selection or phase-switching capability intended to mitigate phase imbalance and increase utilisation of residual capacity. The infrastructure submodel does not prescribe the switching rule. Instead, it defines time-varying phase attachment as an admissible capability that can be activated in the interaction layer.

This separation is deliberate. Phase switching is not just a feature of the device; its value to the system depends on coincident residential loads and the per-phase headroom process. Accordingly, the choice of $\phi(c,t)$ and the assessment of whether switching improves feasibility are treated as part of the electricity system interaction layer, consistent with the broader literature that frames phase selection as an operational decision coupled to network constraints (Ye et al., 2022).

ADMD-based soft headroom constraint in the methodology

In addition to the building's physical intake capacity, the model introduces a "soft headroom" constraint derived from after-diversity maximum demand (ADMD) planning logic. This is intended to preserve secondary transformer and feeder coincident-peak reserves.

The After Diversity Maximum Demand (ADMD) planning construct is used to estimate the peak loading that a low-voltage feeder or distribution transformer is likely to experience when the individual household demands are aggregated and partially offset by

diversity in appliance usage and occupancy patterns. The ADMD "accounts for the coincident peak load that a network is likely to experience over its lifetime" and is "an overestimation of typical demand", reflecting its intended use as a conservative design proxy. In the United Kingdom, low-voltage residential networks are planned in accordance with Engineering Recommendation P2/7. This requires demand to be assessed using after-diversity maximum demand rather than installed service capacity (Energy Networks Association, 2019).

For a domestic customer without electric heating, I mean that the ADMD decreases with the number of customers and stabilises at approximately 1.5 kW per dwelling by the 100th customer, while the uncertainty narrows as the number of customers increases. Public guidance issued by UK Power Networks for new residential developments indicates that domestic dwellings are typically assigned ADMD values of around 1–2 kW under non-electric heating conditions, as determined by the "Customer-Led Network Revolution" (CLNR) project (Barteczko-Hibbert, 2015). Results from EV customers demonstrate that if unmanaged home charging is included in the import, the diversified coincident peak can increase substantially. The whole-house import including EV charging is reported to be around 3.8 kW at the 100th customer. This illustrates why it is pivotal to treat EV charging as "non-random" controllable demand in order to preserve upstream headroom.

Within the current framework, "soft headroom" is defined as the residual coincident-peak capacity implied by ADMD-based upstream reserve calculations. This is distinct from "hard headroom", which is defined by the physical ratings at the building intake, such as the service fuse, rising main ampacity and voltage limits. In operational terms, a building may have a substantial amount of hard headroom at the intake, but the upstream feeder or substation may be close to its diversified coincident peak when the entire downstream portfolio is taken into account.

Because the downstream network is predominantly single-phase, the soft headroom budget is implemented in a phase-resolved manner. For each phase $\phi \in \{a,b,c\}$, a phase soft cap H_{ϕ}^{soft} is allocated proportional to the number of dwellings connected to that phase, and EV charging decisions are constrained so that, at every time interval t, the sum of baseline demand and controlled EV charging on each phase does not exceed its soft cap. This phase-resolved implementation ensures that the controlling constraint reflects the most heavily loaded phase at any given time. This is the relevant condition for low-voltage operation under imbalance, even when the upstream planning metric is expressed as an aggregated diversified peak.

In the context of on-street charging points, these are represented as single-phase assets, which, in essence, draw power on exactly one intake phase in each hour. For each phase $\phi \in \Phi = \{A,B,C\}$ and hour $t \in \mathcal{T}$, the aggregate EV charging power on that phase is defined as the sum of charger-level power draws connected to that phase in that hour:

$$P_{\phi,t}^{EV} = \sum_{c \in \mathcal{C}:\phi(c,t)=\phi} P_{c,t}^{chg}. \quad (14)$$

This definition applies under both a fixed-phase regime, where $\phi(c,t)$ is time-invariant, and a dynamic-phase regime, where $\phi(c,t)$ may vary over time to mitigate phase imbalance and improve utilisation of available capacity. Prior work on adaptive charging networks (Ye et al., 2022) supports the relevance of phase selection and phase optimisation for improving three-phase charging performance.

As this article focuses on technical feasibility rather than behavioural equilibrium, the interaction layer considers charger assignment and, where applicable, phase attachment to be admissible operational degrees of freedom. The only constraints on these degrees of freedom are physical exclusivity of charger use, charger power limits, and the phase import constraints defined in Section 2.2. This distinction clarifies the difference between what is physically feasible and what may arise from specific institutional, market or governance arrangements. These arrangements are intentionally deferred to later work.

For the representative building intake, feasibility is posed as an existence problem. A technically feasible electrification outcome exists if there is at least one set of hourly charger power draws $\{P_{c,t}^{\text{chg}}\}$, charger occupancies, and (where enabled) phase attachment decisions $\{\phi(c,t)\}$ such that charging occurs only within the archetype availability windows, the archetype replenishment requirements are satisfied over the simulation horizon, and the phase import constraints hold for all phases and all hours. According to this definition, the feasibility of on-street charging points is determined by the alignment of residential demand peaks with vehicle availability, as well as by the potential to access residual capacity on individual phases through static allocation and dynamic phase selection.

As an empirical reference point, on-street charging solutions typically offer single-phase AC charging at around 5 kW (25 A at a nominal voltage of 230 V). This is consistent with the bounded-power model described above and establishes a practical “slow charging” baseline for overnight replenishment scenarios. In this paper, such values are used strictly to instantiate the power-limit parameters $P_c^{\max}$; the interaction model itself remains unchanged.

Outputs passed forward

The infrastructure submodule provides the set of charger-level decision objects and constraints needed by subsequent layers: the charger ratings $P_c^{\max}$,

the admissible charging-power variables $P_{c,t}^{\mathrm{chg}}$, the occupancy indicators $x_{c,k,t}$, and the phase-attachment representation $\phi(c,t)$ under either fixed or dynamic regimes. These objects are sufficient for translating the energy requirements and availability windows of archetypes into candidate charging power trajectories. The mapping from candidate trajectories to phase-resolved EV load $P_{\phi,t}^{\mathrm{EV}}$, and the evaluation of feasibility against the per-phase headroom identity $R_{\phi,t}$, and "soft headroom" $H_{\phi,t}^{\mathrm{soft}}$ are undertaken explicitly in the electricity system interaction layer to avoid conflating infrastructure definition with network feasibility assessment.

2.6. Electricity System Interaction and Feasibility Assessment Layer

This layer integrates the baseline residential demand $D_{\phi,t}$, the archetype-derived daily replenishment requirements and charging availability $\{E_{d,k}, A_{k,t}\}$, and the on-street infrastructure representation $\{P_c^{\max}, P_{c,t}^{\mathrm{chg}}, \phi(c,t), H_{\phi,t}^{\mathrm{soft}}\}$ into a phase-resolved interaction model at the building intake. The aim is to establish whether there are any technically acceptable charging schedules that comply with the current low-voltage import limits for a typical multi-occupancy converted terrace house in Kensington.

3. Data and Parameterisation

3.1. The Context of the Case Study and the Scope of the Modelling

The empirical instantiation of the framework was carried out on a representative, multi-occupancy, converted terraced building in Cornwall Gardens, Kensington.

Structural and Historical Context of Cornwall Gardens Electrical Infrastructure

Cornwall Gardens, located in the Royal Borough of Kensington and Chelsea, is a paradigm of high-density, inner-city residential architecture. These properties, which are primarily Victorian and Edwardian townhouses, were originally designed for single-family occupancy by the professional and scientific elite. During the 20th century, these large buildings underwent systematic conversion into multiple self-contained flats. Significant upgrades to the internal electrical distribution systems were required to accommodate increased occupancy while maintaining the integrity of the building's external fabric.

This area is classified as high-density based on planning and monitoring reports detailing the prevalence of self-contained residential flats (Use Class C3) and the intensity of ongoing basement development projects aimed at expanding living spaces. These architectural characteristics directly influence electrical demand: larger flats with high property values tend to have a higher density of appliances, including high-end kitchen equipment, home automation systems and extensive lighting. All of these factors contribute to the "relatively high electricity consumption" noted in the model parameters.

The technical configuration for such buildings usually includes a high-capacity, three-phase, low-voltage (LV) connection from the local distribution network operator (DNO). For this region, the DNO is UK Power Networks (UKPN). Buildings of this type are usually supplied via a three-phase LV intake, with individual flats connected to a single phase via a basement multi-service distribution board (MSDB) (UK Power Networks, 2025a).

Figure 1. A typical Kensington area, with an "over the pavement" charging cable demonstrates lack of public charging options

Main Electrical Infrastructure Assumptions

The most prevalent main fuse rating for such buildings is 3×100 A (UK Power Networks, 2025a), corresponding to a maximum import capacity ("hard limit") of approximately 23 kW per phase. The building is represented as a single low-voltage intake with three phases $\Phi = \{A, B, C\}$ supplying a set of 6 single-phase dwellings $\mathcal{F}$. In accordance with the ADMD phase soft cap H_{ϕ}^{soft} is allocated at 3kW per phase (representing two flats).

The annual household electricity consumption in Cornwall Gardens is significantly higher than the London average. This is due to larger floor areas and the increased continuous baseloads associated with security systems, audiovisual equipment and other permanently energised appliances. Based on empirical evidence from similar properties, the typical annual electricity usage of a flat is assumed to fall within the range of 4,500–6,000 kWh.

Accordingly, the six simulated households are allocated across annual consumption bins as follows:

- One flat in the 2,500–2,999 kWh range;
- two in the 3,000–3,999 kWh range;
- two in the 4,000–4,999 kWh range; and
- one in the 5,000–5,999 kWh range.

This distribution accurately reflects both the average demand level and the observed heterogeneity in high-income, inner-London residential buildings, while remaining conservative with respect to network loading.

3.2. Residential Electricity Demand Data and Processing

Baseline household electricity consumption data is sourced from the Low Carbon London smart meter dataset, which is published via the London Datastore. This dataset comprises half-hourly electricity consumption readings from a sample of 5,567 London households, collected between November 2011 and February 2014. Of these households, approximately 1,100 were exposed to dynamic time-of-use pricing in 2013 (UK Power Networks, 2014).

Because the integrated framework is defined on an hourly time index, half-hourly observations are aggregated to hourly energy consumption. Let $E_{h,\tau}^{(30)}$ denote recorded electricity consumption (kWh) for household h in half-hour interval τ. Hourly baseline demand is constructed as $D_{h,t}^{\text{raw}} = E_{h,2t-1}^{(30)} + E_{h,2t}^{(30)}$, which preserves energy consistency under the adopted discretisation. To avoid contaminating the baseline demand with responses to the induced tariff, the primary specification uses the non-dynamic tariff portion of the sample to construct residential demand profiles, while the dynamic tariff subgroup is reserved for robustness checks as appropriate.

For each retained household h, an annual consumption magnitude A_h is computed and a normalised load shape $s_{h,t} = D_{h,t}^{\text{raw}} / A_h$ is formed to isolate timing from scale. The model then constructs dwelling-level baseline demand $D_{f,t}$ by sampling shapes $s_{h,t}$ from a consumption band judged representative of the case-study dwellings and scaling them to dwelling-level annual targets A_f. This scaling approach is consistent with the recent findings (Rubenis & Laizans, 2026) that once normalised, the residential load shapes in multi-apartment settings exhibit limited systematic divergence across consumption groups. This implies that annual variation is primarily a scale effect rather than a fundamental change in routines.

The mapping of simulations follows the exogenous phase assignment $a(f)$ defined in Section 2.2, and the phase-resolved baseline series $D_{\phi,t}$ is obtained by aggregation.

3.3. Vehicle Archetype Inputs and Energy-Demand Parameterisation

The heterogeneity of vehicle usage is represented using the archetype (cluster) framework, which was previously developed and validated in the authors' fleet electrification study. In this study, archetypes are treated as behavioural primitives that capture distinct patterns of daily distance intensity and temporal availability (Rubenis, Tonova, et al., 2025).

In the present paper, the required data for the feasibility assessment are the daily total driving distance $D_{d,k}$ and daily total driving time $T_{d,k}$ for an archetype k, together with the implied hourly availability indicator $A_{k,t}$ that defines the admissible charging windows.

The daily EV energy demand is constructed using the same WLTP-calibrated mapping previously employed in the charging-access analysis. Specifically, daily total energy consumption is calculated via a speed-weighted interpolation between an urban benchmark and a combined higher-speed benchmark, where average daily speed $v_{d,k} = D_{d,k} / T_{d,k}$ determines the weight through a logistic function. Total daily energy demand $E_{d,k}$ is then computed as the sum of traction energy and a temperature-dependent auxiliary term proportional to driving time (Rubenis, Laizans, et al., 2025). All parameter values for this mapping, including benchmark consumptions and the auxiliary-load specification, are adopted unchanged from the prior study and are therefore reported as part of the parameter table for transparency and replication rather than re-derived in the present article.

3.4. Charging Infrastructure Parameters

On-street charging is modelled as single-phase AC conductive charging equipment with rated power $P_c^{\max}$ (kW) for each charger $c \in \mathcal{C}$. The baseline technology parameterisation is anchored to published specifications for lamppost-based on-street charging, which report a standard maximum charging capacity of 5 kW at 230 V single-phase and 25 A. These specifications explicitly frame this as configurable to local grid conditions. This anchor is used to instantiate $P_c^{\max}$ in the baseline scenario, while sensitivity cases may consider alternative ratings (for example, where 32 A single-phase points are feasible).

The intake capacity parameters $\{P_\phi^{\max}\}$ are instantiated via nominal voltage V^{nom} and phase current limits $I_\phi^{\max}$ as defined in Section 3.2. In designing the scenario, plausible LV supply limits were aligned with UK Power Networks' engineering guidance for LV customer supplies of up to 100 A, as well as the associated maximum apparent power scale. In line with the objective of testing feasibility without upgrades, the import limits are considered external and are not adjusted based on reinforcement decisions in this paper.

Where dynamic phase attachment is examined, phase selection is treated as an operational capability by allowing $\phi(c,t)$ to vary over time, subject to the requirement that each charger is connected to exactly one phase in each hour. This allows the feasibility layer to determine whether phase-resolved spare capacity can be utilised more effectively in the presence of phase imbalance, which is consistent with previous research on phase optimisation in adaptive charging networks.

3.5. Case Design and Feasibility Metrics

The empirical analysis is organised in the form of a scenario grid covering EV penetration and infrastructure provision. Feasibility is evaluated based on the existence of certain conditions. For a given scenario, the system is deemed technically feasible if there exists at least one assignment of vehicles to chargers and one hourly charging-power trajectory $\{P_{c,t}^{\text{chg}}\}$ that (i) respects charger power bounds, (ii) charges only in hours where the relevant archetype is available, (iii) satisfies replenishment requirements implied by $\{E_{d,k}\}$ over the simulation horizon, and (iv) maintains compliance with the phase import limits $L_{\phi,t} \le P_\phi^{\max}$ for all ϕ and t. Results are reported using feasibility indicators at the scenario level and diagnostic measures that characterise the limiting factors, including the distribution of phase headroom $R_{\phi,t}$ and the frequency with which replenishment requirements bind within available overnight windows.

The parameters that define the baseline case and the sensitivity ranges are summarised in Table 1. Values adopted unchanged from previous studies are labelled as such, emphasising that the present manuscript's contribution lies in integration and feasibility evaluation rather than the reinvention of component models.

4. Results

4.1. Headroom Modelling results

To represent typical energy consumption in a terraced house in Kensington, London, six households were simulated across the selected consumption bins.

The model's representation of household electricity demand is shaped by winter-dominated seasonal variability and a pronounced concentration of demand in the evening. The periods of lowest system stress consistently occur during the night-time and in the late summer to early autumn months, while the most constrained periods coincide with winter evenings. These empirically derived demand structures provide the basis for assessing additional electrification loads, including electric vehicle charging, in the subsequent sections of the paper.

Two allocation methods were used to distribute flats across three phases: an optimal method, which aimed to make consumption similar across all three phases, and a worst-case method, which involved assigning the two largest consumers to one phase to create maximum imbalance between phases. The headrooms were calculated for each phase based on ADMD phase soft cap H_ϕ^{soft} of 3kW per phase.

The average headrooms varied from 1.2 to 2.4 kW for the optimised phase allocation and from 0.7 to 1.5 for the worst-case scenario, however in the case of the latter, there were significant differences between headrooms for individual phases.

In the worst-case scenario, the differences were up to 2.5 times higher (see Figure 4). This also resulted in differences in available headroom (see Figure 5), which includes frequent negative headroom. In other words, the energy consumption is higher than estimated after the maximum demand diversity (ADMD), even without adding electric vehicle chargers.

Examining the distribution of headroom, it can be seen that on most days, the available size of headroom lies between 1.5 and 2 kW across all phases. There is also a shift between phases: the loss of headroom in the phase with the highest consumption is compensated for by the phase with the lowest.

4.2. Charging modelling

The headroom distribution shows that there is no practical benefit to increasing the charger's power

Table 1

Parameterisation for the empirical case

Parameter	Symbol	Baseline value	Sensitivity range / scenarios	Source / rationale
Time step	Δt	1 hour	fixed	Section 3.2 definition
Horizon	T	8,760	fixed	Section 3.2 definition
Number of dwellings in representative building	$\mathcal{F}$	6	fixed	Case study
Nominal phase voltage	V^{nom}	230 V	fixed	LV nominal supply representation; consistent with UK practice
Phase current limit at intake	$I_{\phi}^{\max}$	60A	60–100 A per phase (scenarios)	UKPN LV supplies guidance
Per-phase import limit	$P_{\phi}^{\max}$	$V^{\text{nom}} I_{\phi}^{\max}$	implied	Section 3.2 identity
Number of on-street chargers serving the building	$\mathcal{C}$	2	1-2	
Charger rated power	$P_{c}^{\max}$	5 kW	3.6 - 7.2 kW	
Phase attachment regime	$\phi(c,t)$	fixed	fixed vs dynamic	Dynamic phase selection literature
Household demand data	$D_{h,t}^{\text{raw}}$	LCL smart meter	fixed	London Datastore LCL dataset
Normalised household shape	$s_{h,t}$	$D_{h,t}^{\text{raw}} / A_h$	implied	Section 4.2; shape invariance evidence (Rubenis, Laizans, et al., 2025)
Archetype set	$\mathcal{K}$	Parameterisation for the empirical case	fixed	Prior datasets used in archetype modelling (Rubenis, Tonova, et al., 2025)
Daily distance input	$D_{d,k}$		fixed	Prior datasets used in archetype modelling (Rubenis, Tonova, et al., 2025)
Daily driving time input	$T_{d,k}$		fixed	Prior datasets used in archetype modelling (Rubenis, Tonova, et al., 2025)
Energy mapping	$E_{d,k}$	Eq. (11)	fixed	Adopted from prior access study (Rubenis, Laizans, et al., 2025).

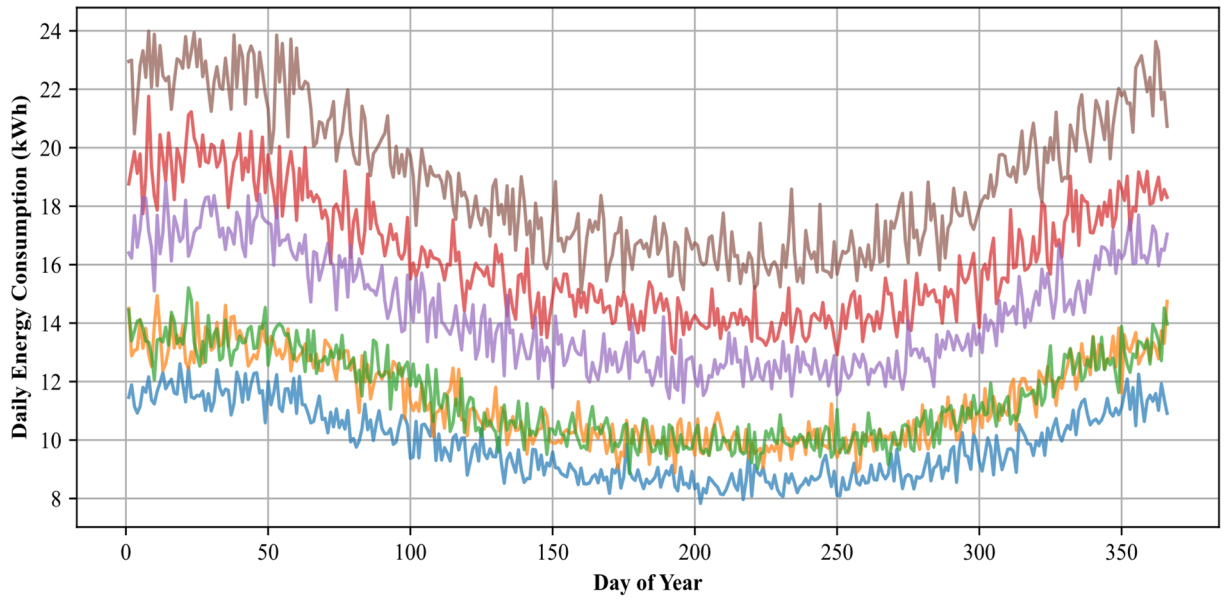

Figure 2. Simulated energy consumption in 6 flats

above standard slow charging (3.6 kWh), as at no point is there enough free headroom to justify it.

Charging was modelled under six scenarios: 1, 2 and 3 cars with optimal and worst-case phase connection options. This was done to assess whether vehicle charging could meet the simulated energy consumption of EVs. The main simulation results are shown in Table 2.

The achieved battery state of charge (SoC) distributions across all six scenarios indicate that the system can generally maintain relatively high average charge levels for vehicles over the full 366-day simulation horizon, even under the strict after-diversity maximum demand (ADMD) constraint of 3.0 kW per phase. In the case of a single vehicle, the mean SoC remains at around 70–73% of the nominal capacity. The *worst-phase* configuration yields a slightly higher mean SoC (approximately 43.6 kWh, or 72.7%) than the *optimal-phase* configuration (approximately 42.1 kWh, or 70.1%). This counterintuitive result reflects the fact that phase allocation does not introduce binding competition effects when only one vehicle is present; instead, small differences in phase headroom timing can marginally increase charging availability in the worst-case scenario without causing congestion. Notably, the maximum SoC consistently reaches the full usable capacity of 60 kWh in both cases, while the minimum SoC values drop to approximately 4.6–5.9 kWh. This suggests that the vehicle occasionally operates close to deep discharge, but can subsequently recover.

As the number of vehicles increases to two or three, phase allocation becomes much more important, and the differences between the optimal and worst configurations become clearer at fleet level. With optimal phase allocation, the mean SoC values remain relatively balanced between vehicles, usually ranging from 63% to 70% of capacity, even in the case of three vehicles. In contrast, the worst-phase scenarios demonstrate a consistent increase in dispersion. While the first vehicle maintains a relatively high mean SoC of around 72.7%, subsequent vehicles experience lower averages. This is particularly evident in the three-vehicle worst-case scenario, where the third vehicle's mean SoC decreases to approximately 36.7 kWh (61.2%). This is accompanied by higher standard deviations and lower minimum SoC values, indicating more frequent and severe excursions into low-charge states due to increased competition for limited per-phase capacity. Overall, the results demonstrate that, in the case of multiple vehicles, suboptimal phase connections do not result in complete charging

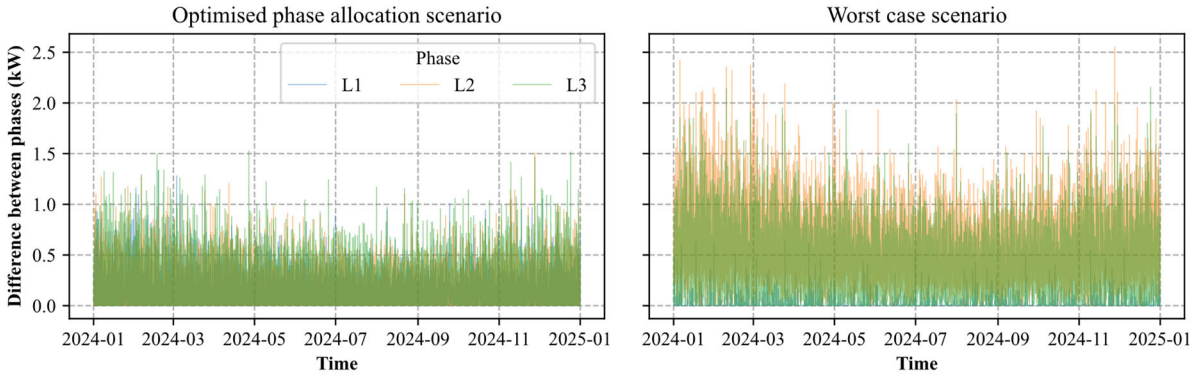

Figure 3. Differences in available headrooms in different scenarios

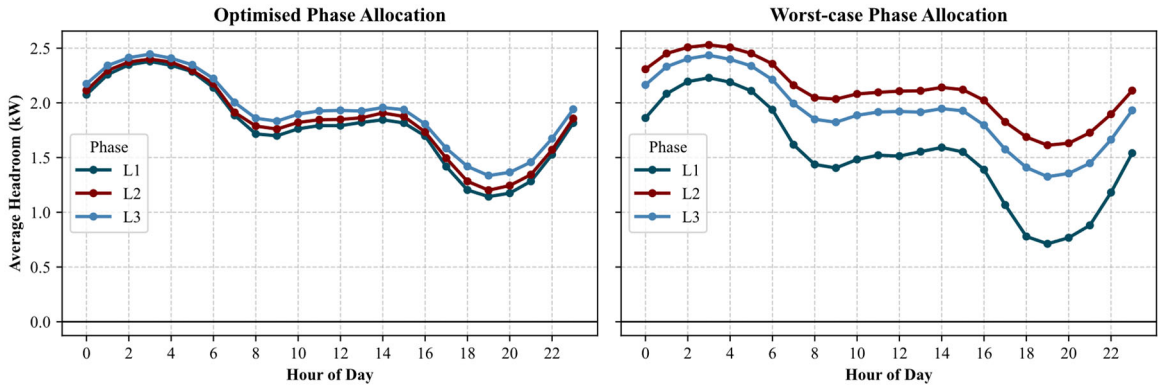

Figure 4. The distribution of the available headrooms in different scenarios

Table 2
EV Battery State of Charge Simulation

Scenario	Number of vehicles	Vehicle ID	Mean SoC (kWh)	Mean SoC (%)	Min SoC (kWh)	Std. dev. (kWh)
1car_opt	1	c0_001	42.07	70.10%	4.61	15.69
1car_worst	1	c0_001	43.63	72.70%	5.89	15.15
2cars_opt	2	c0_001	42.07	70.10%	4.61	15.69
		c0_002	37.92	63.20%	4.07	16.02
2cars_worst	2	c0_001	43.63	72.70%	5.89	15.15
		c0_002	38.81	64.70%	4.57	15.77
3cars_opt	3	c0_001	42.07	70.10%	4.61	15.69
		c0_002	37.92	63.20%	4.07	16.02
		c0_003	39.52	65.90%	7.31	16.44
3cars_worst	3	c0_001	43.63	72.70%	5.89	15.15
		c0_002	38.81	64.70%	4.57	15.77
		c0_003	36.71	61.20%	5.24	17.29

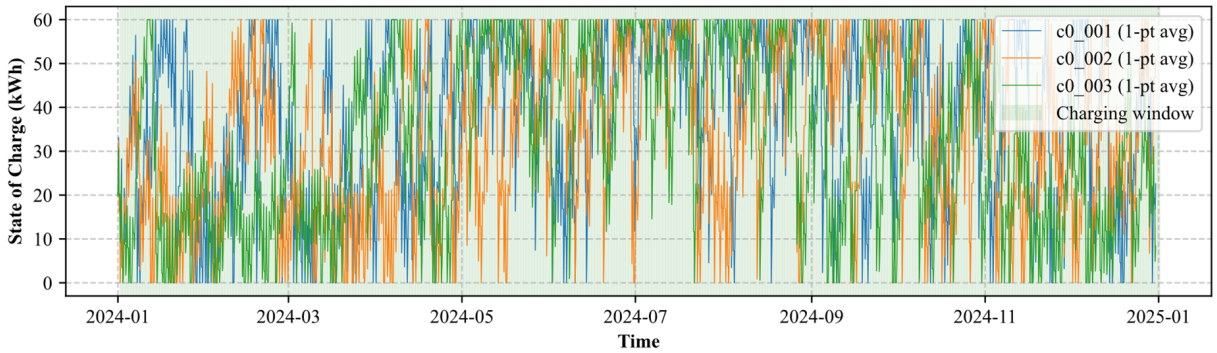

Figure 5. The EV SoC after the charging, while keeping within 3kW ADMD limit

failure. While maximum SoC still reaches full capacity, charging opportunities are redistributed unevenly across vehicles, leading to a lower average SoC and greater variability for some users. This emphasises the importance of phase allocation in ensuring charging equity and reliability when multiple EVs share limited residential electrical infrastructure.

4.3. Effect on Grid Quality

Interestingly, the opposite effect is seen on grid quality: the best results are achieved in three-vehicle scenarios with chargers connected to all three phases.

In the single-vehicle case, phase imbalance is relatively high in absolute terms, with mean charge imbalance values of around 2.05 kW and 2.15 kW in the optimal and worst scenarios, respectively. However, from a system perspective, this imbalance is largely inconsequential, as the mean total charging power remains low (around 2.05–2.15 kW), and a substantial amount of capacity remains unused. In both cases, the mean unused capacity exceeds 4.28 kW. The difference between the optimal and worst phase allocations mainly manifests as a marginal increase in the total energy delivered in the worst case rather than as a structural efficiency gain.

As the number of vehicles increases from one to two, the total charging activity intensifies. This is reflected in a higher mean total charging power of approximately 3.62–3.69 kW, as well as a sharp reduction in unused capacity to around 2.52–2.59 kW. In this scenario, the mean charge imbalance remains high, exceeding 2.1 kW in both cases. The worst-phase configuration exhibits a slightly higher imbalance than the optimal configuration. At the same time, the total energy delivered is slightly higher under worst-phase allocation. This suggests that a higher degree of imbalance does not necessarily result in a lower aggregate energy throughput when the system has not yet reached full saturation. However, increased imbalance coincides with reduced flexibility, as evidenced by declining unused capacity.

Qualitatively different behaviour emerges in the three-vehicle scenarios. Optimal phase allocation results in a significant reduction in mean charge imbalance, which falls to around 0.95 kW. This is in contrast to the worst-phase configuration, which results in a mean charge imbalance of 1.18 kW. This improvement in energy consumption balance occurs in 66% of hours. This reduction occurs alongside the near-full utilisation of available capacity, with the mean unused capacity dropping to around 1.0 kW in both cases,

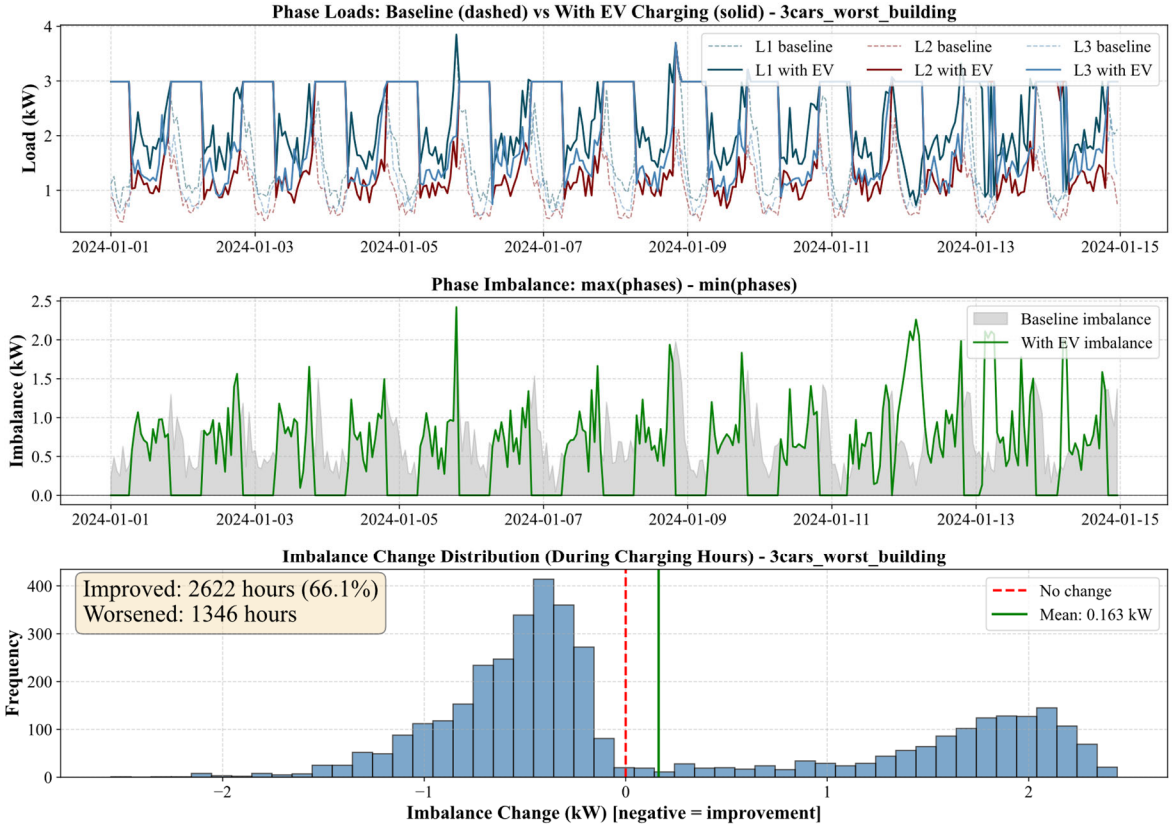

Figure 6. The controlled EV charging effect on grid, keeping consumption of each phase within 3kW ADMD limit

while the mean total charging power exceeds 5.1 kW. Importantly, the total energy delivered over the simulation horizon is almost identical in the optimal and worst-case scenarios. This indicates that, in the saturated regime, phase optimisation primarily redistributes load more evenly across phases rather than increasing the total energy throughput. The results therefore suggest that under high utilisation conditions, optimal phase allocation significantly improves balance and operational symmetry without necessarily increasing the total energy delivered, whereas under lower utilisation conditions, imbalance plays a less significant role in relation to overall capacity availability.

5. Discussion

The results clearly demonstrate the practical feasibility of on-street residential charging in areas with limited low-voltage distribution capacity. At low to moderate levels of EV penetration, the findings suggest that on-street charging can be operationally viable without the need for immediate network reinforcement, provided charging points are distributed across multiple buildings or feeder segments. In such configurations, spreading chargers across space can increase the effective maximum demand available to each vehicle after demand has been diversified, thereby reducing direct competition for phase-limited capacity. This mechanism is reflected in the relatively high mean state of charge and lower incidence of insufficient charging observed in the single- and two-vehicle scenarios. From a systems perspective, this suggests that substation upgrades are not an inherent requirement of early-stage on-street electrification. Instead, careful allocation of chargers across homes and phases can significantly improve charging outcomes by increasing the probability that vehicles reach a high state of charge overnight.

However, the results also suggest that this strategy has clear limitations. As the number of electric vehicles approaches saturation – defined here as the point at which they represent a significant proportion of all parked vehicles rather than a small minority – the system transitions into a capacity-constrained regime. In the three-vehicle scenario, the proportion of days with a morning state of charge below 50% converges to around one third, regardless of the phase optimisation strategy. This suggests that optimisation alone can no longer offset the structural limitations imposed by the fixed ADMD constraint.

The incidence of days with an insufficient morning charge (defined as a state of charge below 50%) reveals a clear dependence on fleet size, as well as a more nuanced dependence on phase allocation strategy.

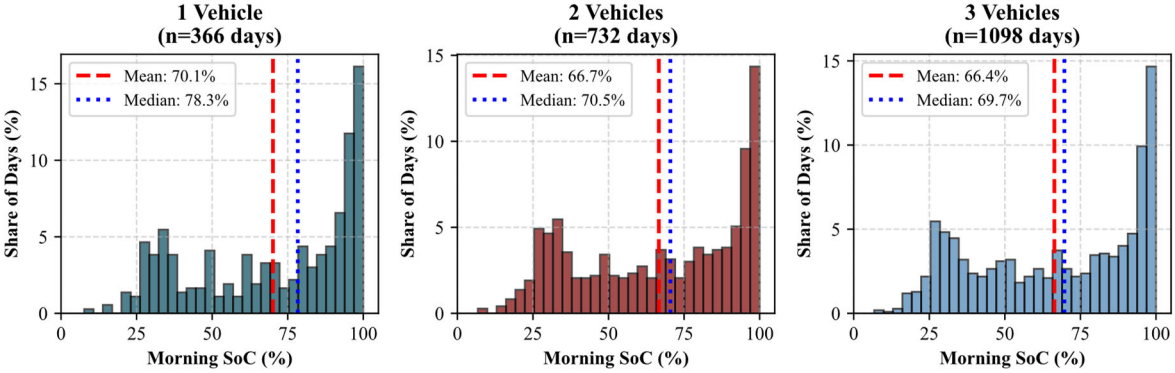

Figure 7. The distribution of the SoC in the morning

In single-vehicle scenarios, the proportion of days with an SoC below 50% remains below one-third of all observed days. Under optimised phase allocation, insufficient charge occurs on 28.4% of days, whereas the worst-case phase configuration exhibits a slightly lower proportion at 24.9%. This mirrors earlier results showing that, in the absence of competition for capacity, phase allocation does not act as a binding constraint and can marginally increase charging availability through the coincidental alignment of headroom. In line with this, the worst-case single-car scenario achieves a higher mean SoC of 72.7%, compared to 70.1% under optimisation.

As the number of vehicles increases, the frequency of mornings with insufficient charge rises markedly. With two vehicles, the proportion of days with an SoC below 50% increases to 32.5% under optimised phase allocation and to 29.9% under worst-case allocation, despite mean SoC values remaining relatively high at 66.7% and 68.7%, respectively. This suggests that the average charge level masks an increasing tail risk: although vehicles are usually charged to around two-thirds of their maximum capacity, many days still begin with limited usable range. The difference between the mean state of charge (SoC) and the frequency of low SoC mornings highlights the growing importance of intra-fleet competition and temporal coincidence effects, as more vehicles share limited charging infrastructure.

In three-vehicle scenarios, the system enters a clearly capacity-constrained regime. The proportion of days with a morning SoC below 50% amounts to around one third of all observations in both phase configurations, reaching 33.1% under optimisation and 33.9% under worst-case allocation. At this utilisation level, the differences between the phase strategies in terms of sufficiency outcomes largely disappear, even though optimisation continues to improve balance and equity in other dimensions. Mean SoC values also converge to 66.4% and 66.2%, respectively. These results suggest that phase optimisation alone is insufficient to materially reduce the probability of low-charge mornings once residential charging approaches saturation under a fixed ADMD limit. Rather, structural measures such as higher connection capacity, additional charging windows or explicit prioritisation rules would be necessary to enhance reliability for all users.

At this stage, improvements in phase balance and utilisation efficiency redistribute available energy more equitably across vehicles, rather than increasing the overall sufficiency of charging. This

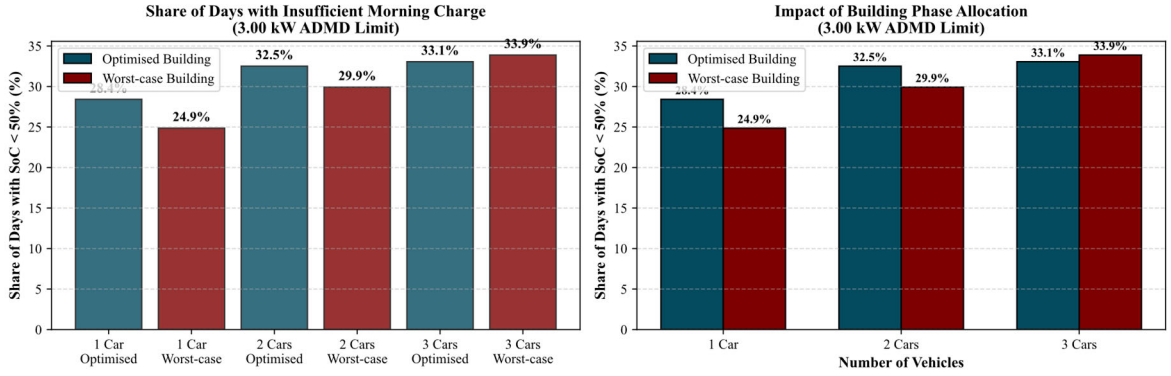

Figure 8. The insufficiency of SoC in the morning (less than 50% of battery capacity)

suggests that, beyond a certain threshold of EV penetration, further growth in on-street EV charging cannot be accommodated solely through smarter use of existing infrastructure, and that increases in substation or feeder capacity will be required.

These findings highlight an important distinction between the *efficiency-* and *capacity-led* phases of electrification. In the early phase, optimisation, spatial diversification of chargers and demand coordination can deliver significant improvements in user outcomes without the need for capital-intensive grid upgrades. However, in the later phase, the binding constraint becomes total available capacity rather than its allocation. Addressing this constraint may require a combination of traditional reinforcement methods and more advanced flexibility mechanisms. In this context, vehicle-to-grid operation emerges as a promising area for future analysis. Allowing vehicles to act as both loads and distributed storage resources could enable vehicle-to-grid technology to partially relax effective capacity constraints during critical periods and reduce the frequency of low-charge mornings. The next logical step in the analysis is to evaluate whether such bidirectional operation could significantly extend the feasible range of on-street charging without extensive grid upgrades.

6. Conclusions

The results indicate that, for a representative multi-occupancy terraced building under an ADMD-derived phase soft cap, the binding constraint for on-street slow AC charging is not the charger's nominal rating, but the remaining "soft headroom" after coincident residential demand has been accounted for. In the empirical case, the available headroom is most frequently in the low kilowatt range. This implies that increasing the charger power above the standard slow charge level is not very practical because the upstream coincident peak budget cannot support a higher sustained draw.

In a simulated setting with low to moderate EV penetration (one to two vehicles), the system can generally achieve high overnight state-of-charge outcomes without the need for immediate distribution upgrades, provided charging points are spatially diversified and phase exposure is managed to prevent vehicles from competing for the same phase-limited capacity. However, as utilisation approaches saturation (three vehicles in the modelled building context), the probability of low-charge mornings increases markedly, converging to around one-third of days. In this case, phase optimisation primarily improves the balance and equity of allocation rather than increasing the total energy delivered.

These findings suggest a two-stage electrification process for dense urban on-street environments. While early progress can be made through operational coordination and phase-aware allocation, higher levels of penetration ultimately require structural flexibility or reinforcement to ensure reliability for all users. Further research will extend the model to include vehicle-to-grid (V2G) operations and AI-enabled charging management in order to evaluate whether it is possible to achieve additional efficiency gains and reliability improvements under the same distribution constraints.

Acknowledgement

This paper has been published within the research project "Development of a prototype of an environmentally friendly electric car charging ecosystem by integrating renewable energy sources and balancing the power grid", a grant programme financed by the European Recovery Fund and managed by Latvian Central Finance and Contracting Agency. Project number: 2.2.1.3.i.0/1/24/A/CFLA/004.

Author's Contributions

A.R. conducted the main research and analysis. A.L. provided methodological guidance and critically reviewed the manuscript. G.A. was responsible for securing financial support for the research and dataset preparation.

References:

Anadón Martínez, V., & Sumper, A. (2023). Planning and operation objectives of public electric vehicle charging infrastructures: A review. *Energies, 16*(14), 5431.

Barteczko-Hibbert, C. (2015). *After Diversity Maximum Demand (ADMD) Report* (CLNR-L217; p. 24). Northern Powergrid (Northeast) Limited. http://www.networkrevolution.co.uk/project-library/diversity-maximum-demand-admd-report/

Doda, D. K., Beemkumar, N., Awasthi, A., & Gautam, A. K. (2024). *Electric Vehicle Energy Management: Charging in Sustainable Urban Settings for Smart Cities. 540*, 02022.

Energy Networks Association. (2019). *Engineering Recommendation P2/7—Security of Supply* (Engineering Recommendation P2; Version 7). Energy Networks Association. https://www.dcode.org.uk/assets/files/Qualifying%20Standards/ENA_EREC_P2_Issue%207_(2019).pdf

European Commision. (2025). *REPowerEU - 3 years on*. https://energy.ec.europa.eu/topics/markets-and-consumers/actions-and-measures-energy-prices/repowereu-3-years_en

International Electrotechnical Commission. (2017). *IEC 61851-1:2017 Electric vehicle conductive charging system—Part 1: General requirements* (61851; Version 1:2017). International Electrotechnical Commission. https://webstore.iec.ch/en/publication/33644

Ivanova, A., Chassin, D., Aguado, J., Crawford, C., & Djilali, N. (2020). Techno-economic feasibility of a photovoltaic-equipped plug-in electric vehicle public parking lot with coordinated charging. *IET Energy Systems Integration*, *2*(3), 261–272.

Office for Zero Emission Vehicles. (2025). *Apply for the electric vehicle (EV) pavement channels grant*. GOV.UK. https://www.gov.uk/guidance/apply-for-the-electric-vehicle-ev-pavement-channels-grant

Regulation (EU) 2021/1119 of the European Parliament and of the Council of 30 June 2021 Establishing the Framework for Achieving Climate Neutrality and Amending Regulations (EC) No 401/2009 and (EU) 2018/1999 ('European Climate Law'), 2021/1119, European Parliament (2021). https://eur-lex.europa.eu/eli/reg/2021/1119/oj/eng

Rubenis, A., & Laizans, A. (2026). Residential electricity demand structure in multi-apartment buildings: Implications for rooftop photovoltaic availability and urban energy resilience. *Baltic Journal of Economic Studies*, *12*(2). https://doi.org/10.30525/2256-0742/2025-11-5-126-138

Rubenis, A., Laizans, A., & Aleksans, G. (2025). (Pre-print) The Cost of Access: Economic Inequality in On-Street Electric Vehicle Charging in Riga and London. *International Multidisciplinary Scientific GeoConference Surveying Geology and Mining Ecology Management, SGEM*, *25*.

Rubenis, A., Tonova, J., & Morozovs, V. (2025). Modelling Operational Archetypes for Corporate Fleet Electrification. *Baltic Journal of Economic Studies*, *11*(5), 126–138. https://doi.org/10.30525/2256-0742/2025-11-5-126-138

Sastry, K. V., Taylor, D. G., & Leamy, M. J. (2023). Decentralized smart charging of electric vehicles in residential settings: Algorithms and predicted grid impact. *IEEE Transactions on Smart Grid*, *15*(2), 1926–1938.

Schofield, J. R., Carmichael, R., Tindemans, S., Bilton, M., Woolf, M., & Strbac, G. (2015). Low carbon london project: Data from the dynamic time-of-use electricity pricing trial, 2013. *uK Data Service, SN*, *7857*(2015), 7857–7851.

Teawnarong, A., Angaphiwatchawal, P., & Chaitusaney, S. (2024). Optimal operations of local energy market with electric vehicle charging and incentives for local grid services. *IEEE Access*.

Tveit, M. H., Sevdari, K., Marinelli, M., & Calearo, L. (2022). *Behind-the-meter residential electric vehicle smart charging strategies: Danish cases. 1*, 1–5.

Ubitricity. (2025). AC Lamppost Chargers. *Ubitricity*. https://ubitricity.com/en/charging-solutions/ac-lamppost/

UK Power Networks. (2014). *SmartMeter Energy Consumption Data in London Households* [Csv]. London Datastore. https://data.london.gov.uk/dataset/smartmeter-energy-consumption-data-in-london-households-vqm0d

UK Power Networks. (2025a). *BNO Guide An overview of multi-occupied buildings and Building Network Operators (BNOs)* (V4). UK Power Networks. https://media.umbraco.io/ukpn-cms/fj5i0udr/uk-power-networks-bno-guide-2025.pdf

UK Power Networks. (2025b). *EDS 08-2101 LV Customer Supplies up to 100A* (ENGINEERING DESIGN STANDARD EDS 08-2101; Version 14). https://g81.ukpowernetworks.co.uk/library/design-and-planning/lv/eds-08-2101-lv-customer-supplies-up-to-100a

Ye, Z., Li, T., & Low, S. (2022). Towards balanced three-phase charging: Phase optimization in adaptive charging networks. *Electric Power Systems Research*, *212*, 108322. https://doi.org/10.1016/j.epsr.2022.108322

Zhang, G., Tan, S. T., & Wang, G. G. (2017). Real-time smart charging of electric vehicles for demand charge reduction at non-residential sites. *IEEE Transactions on Smart Grid*, *9*(5), 4027–4037.

Received on: 10th of February, 2026
Accepted on: 13th of May, 2026
Published on: 03rd of July, 2026